## Supporting Information

# In Search of Selectivity in Inhibition of ADAM10

Kiran V. Mahasenan,[†] Derong Ding,[†] Ming Gao,[†] Trung T. Nguyen,[†] Mark A. Suckow,[‡] Valerie A. Schroeder,[‡] William R. Wolter,[‡] Mayland Chang,[†]* and Shahriar Mobashery[†]*

†Department of Chemistry and Biochemistry, University of Notre Dame, Notre Dame, Indiana 46556, USA. ‡Freimann Life Science Center, University of Notre Dame, Notre Dame, Indiana 46556, USA.

*S.M.: E-mail, mobashery@nd.edu; Phone, +1-574-631-2933
*M.C.: E-mail, mchang@nd.edu, Phone, +1-574-631-2965

### Table of contents

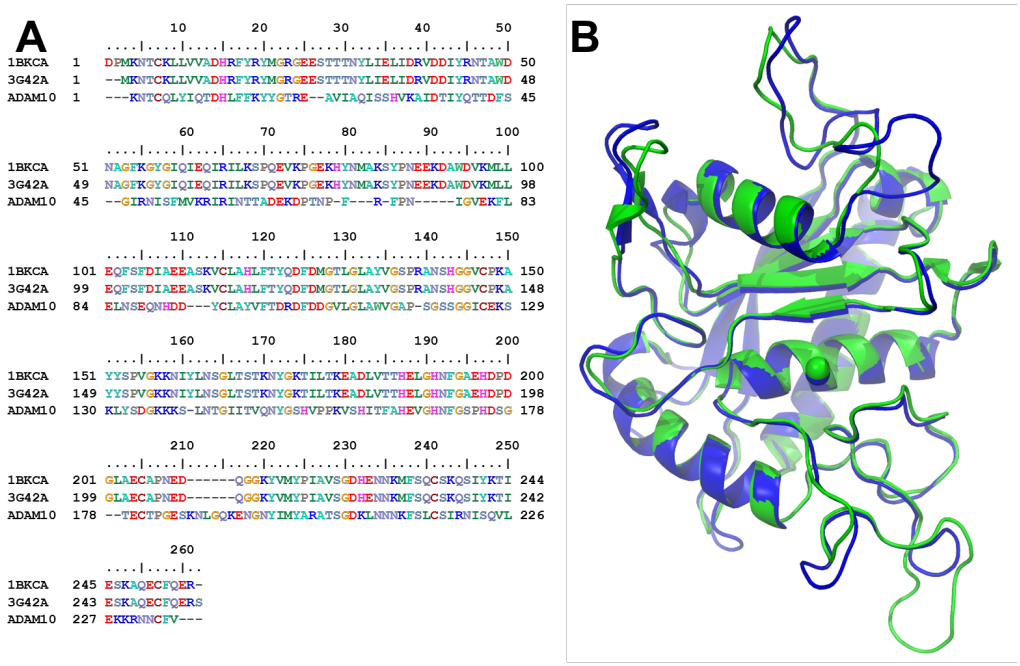


**Figure S1**. (A) Sequence alignment of ADAM10 catalytic domain with templates of ADAM17 (PDB IDs 1BKC and 3G42; sequence identity and similarity are 35% and 52% respectively). (B) ADAM10 model (green) superimposed with the ADAM17 crystal structure (blue) shows the high conservation of the structure, with variations at a few regions in the peripheries of the structure.

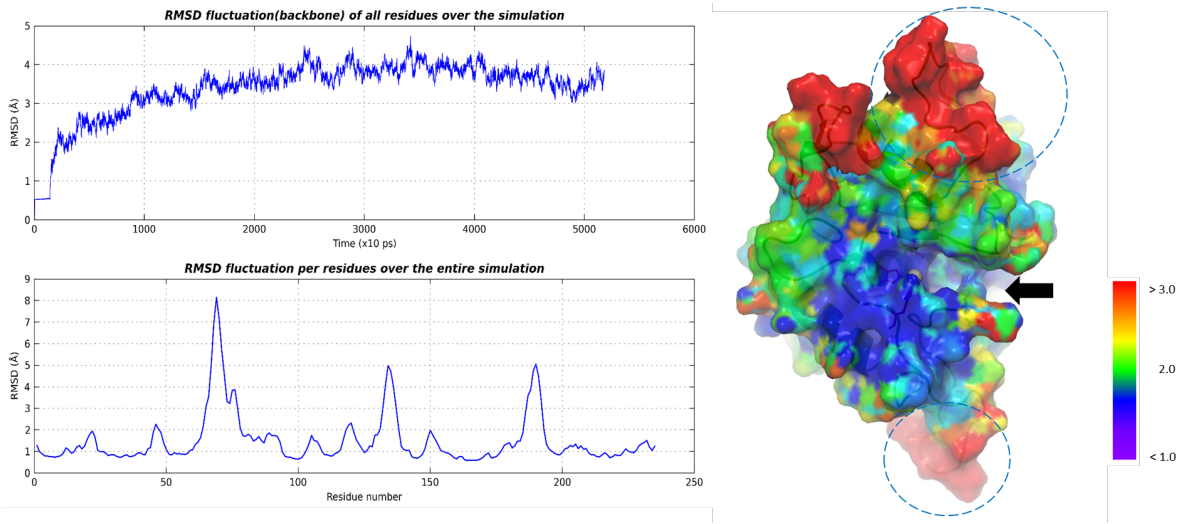


**Figure S2**. RMSD fluctuation of the backbone of the ADAM10 computational model as a function of time during molecular dynamics and the regions of flexibility. To the right, the extent of dynamics of the protein is represented by color scale of RMSD in Å on the protein surface. Most dynamics was observed on two regions (in blue circle) away from the active-site groove (indicated by the arrow).

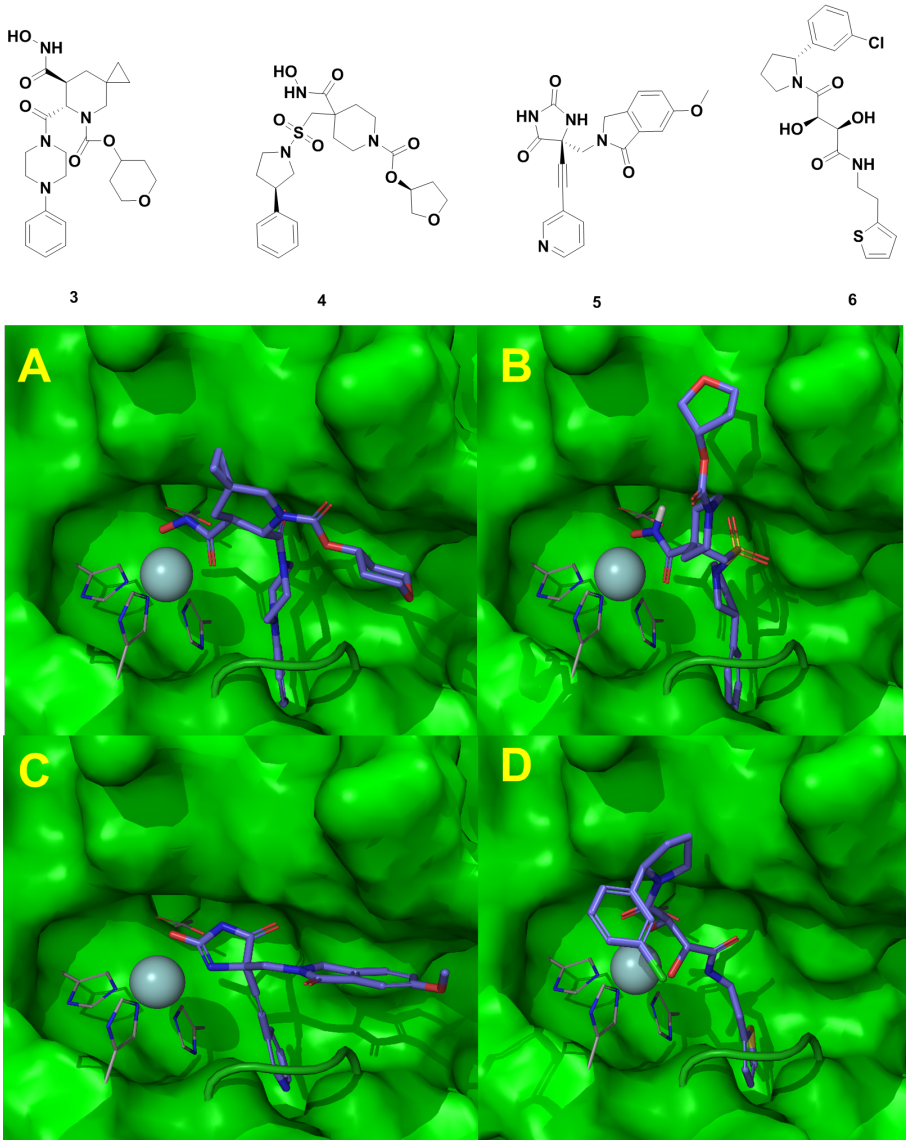


**Figure S3**. The chemical structures of four selected ADAM10 inhibitors[1-4], each from diverse chemical classes (Top panel). The docked binding pose of the compounds (stick representation, carbon atoms in purple) to the active site of the model as calculated by Glide XP docking program (bottom panel, A to D correspond to the models for binding of compounds **3**, **4**, **5**, **6**, respectively). Compound **3** and **4** chelate with zinc-ion via the hydroxamates. The compounds bind in the groove that recognize the substrate.

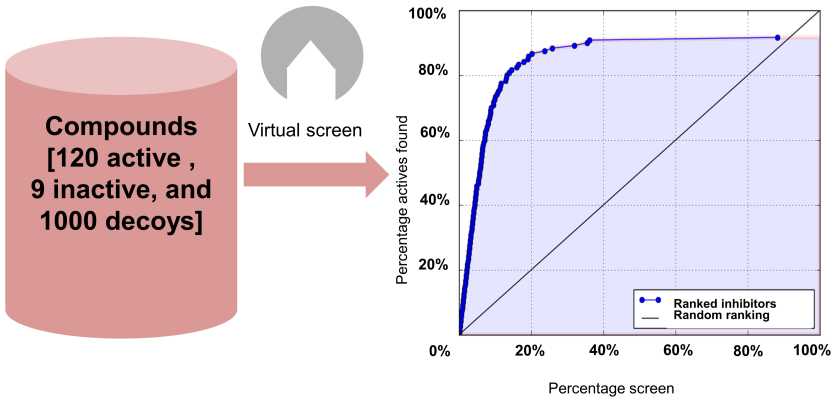


**Figure S4**. Molecular docking enrichment study with the ADAM10 computational model. More than 80% of the active compounds were ranked within the top 20% of the scored library. The ADAM10 active ($K_i$/$IC_{50}$ ≤ 1 μM) and inactive (or less active) compounds ($K_i$/$IC_{50}$ > 5 μM) were obtained from BindingDB (www.bindingdb.org).[5] The decoy set of 1000 compounds were obtained from Schrödinger LLC, USA.[6]

**Table S1: Enzyme inhibition data of compounds obtained from BindingDB[5] (www.bindingdb.org) showing cross-reactivity of ADAM10 inhibitors to MMP-2 and MMP-9 ($IC_{50}$ in nM)[1, 7-10]**

| COMPOUND ID | ADAM10 | MMP-2 | MMP-9 |
|---|---|---|---|
| BINDINGDB_50203524 | 310 | 150 | >5000 |
| BINDINGDB_50203529 | 118 | 195 | 650 |
| BINDINGDB_50203530 | 110 | >1000 | >5000 |
| BINDINGDB_50203534 | 310 | 150 | >5000 |
| BINDINGDB_50203535 | 330 | 350 | >5000 |
| BINDINGDB_50203537 | 137 | 446 | >5000 |
| BINDINGDB_50227984 | 1102 | >5000 | NA |
| BINDINGDB_50227994 | 27 | 86 | 1499 |
| BINDINGDB_50227995 | 194 | 391 | 604 |
| BINDINGDB_50227997 | 139 | 1387 | NA |
| BINDINGDB_50228001 | 26 | 106 | 2623 |
| BINDINGDB_50228003 | 38 | 5 | NA |
| BINDINGDB_50228004 | 14 | 32 | NA |
| BINDINGDB_50228005 | 184 | 63 | 1268 |
| BINDINGDB_50228005 | 184 | 63 | 1268 |
| BINDINGDB_50265157* | 97 | >5000 | >5000 |
| BINDINGDB_50268906 | 19 | 8 | NA |
| BINDINGDB_50268951 | 167 | 92 | NA |
| BINDINGDB_50268952 | 77 | 81 | NA |
| BINDINGDB_50268953 | 1545 | 180 | NA |
| BINDINGDB_50268954 | 196 | 106 | 577 |
| BINDINGDB_50268999 | 64 | 271 | 1443 |
| BINDINGDB_50269000 | 58 | 321 | 1876 |
| BINDINGDB_50269001 | 30 | 68 | >2500 |
| BINDINGDB_50269002 | 83 | 236 | NA |
| BINDINGDB_50269056 | 111 | 156 | NA |
| BINDINGDB_50269057 | 15 | 100 | 683 |
| BINDINGDB_50269058 | 165 | 1090 | NA |
| BINDINGDB_50301102 | 20 | 432 | >5000 |
| BINDINGDB_50301109 | 11 | >2000 | >5000 |
| BINDINGDB_50301113 | 18 | 471 | >5000 |
| BINDINGDB_50301115 | 58 | 730 | >5000 |
| BINDINGDB_50301118 | 9.6 | 344 | >5000 |
| BINDINGDB_50301119 | 35 | 843 | >5000 |
| BINDINGDB_50301120 | 26 | 1475 | >5000 |

* Reported activity data for compound **1**. NA, data not available

**Table S2**. Comparison of amino-acid residues of active sites of ADAM10 model with those of MMP2, MMP9, and ADAM17 based on the structural superposition of X-ray structures (PDB IDs, ICK7, 2OVX, and 1BKC respectively) to the model. Residues at the S1 site, which often determine selectivity, are highlighted in bold letters.

| *Index number* | *ADAM10* | *MMP2* | *MMP9* | *ADAM17* |
|---|---|---|---|---|
| *1* | **VAL297** | **PHE184** | **PRO180** | **VAL314** |
| *2* | GLU298 | TYR182 | TYR179 | LYS315 |
| *3* | **PHE323** | **GLY186** | **ASP182** | **PHE343** |
| *4* | ASP324 | ASP185 | ASP182 | ASP344 |
| *5* | **ASP325** | **GLY189** | **GLY186** | **MET345** |
| *6* | GLY326 | GLY189 | GLY186 | GLY346 |
| *7* | **VAL327** | **LEU190** | **LEU187** | **THR347** |
| *8* | LEU328 | LEU191 | LEU188 | LEU348 |
| *9* | GLY329 | ALA192 | ALA189 | GLY349 |
| *10* | LEU330 | HID193 | HID190 | LEU350 |
| *11* | ALA331 | ALA194 | ALA191 | ALA351 |
| *12* | ILE379 | LEU399 | LEU397 | LEU401 |
| *13* | THR380 | VAL400 | VAL398 | VAL402 |
| *14* | ALA382 | ALA402 | ALA400 | THR404 |
| *15* | HIS383 | HIS403 | HIS401 | HIS405 |
| *16* | GLU384 | GLU404 | GLU402 | GLU406 |
| *17* | HIS387 | HIS407 | HIS405 | HIS409 |
| *18* | HIS393 | HIS413 | HIS411 | HIS415 |
| *19* | ASN414 | GLY418 | GLU416 | LYS432 |
| *20* | TYR415 | ALA419 | ALA417 | TYR433 |
| *21* | ILE416 | LEU420 | LEU418 | VAL434 |
| *22* | MET417 | MET421 | MET419 | MET435 |
| *23* | TYR418 | ALA422 | TYR420 | TYR436 |
| *24* | ALA419 | PRO423 | PRO421 | PRO437 |
| *25* | ARG420 | ILE424 | MET422 | ILE438 |
| *26* | ALA421 | TYR425 | TYR423 | ALA439 |
| *27* | THR422 | THR426 | ARG424 | VAL440 |
| *28* | ASN429 | PHE431 | PRO430 | ASN447 |

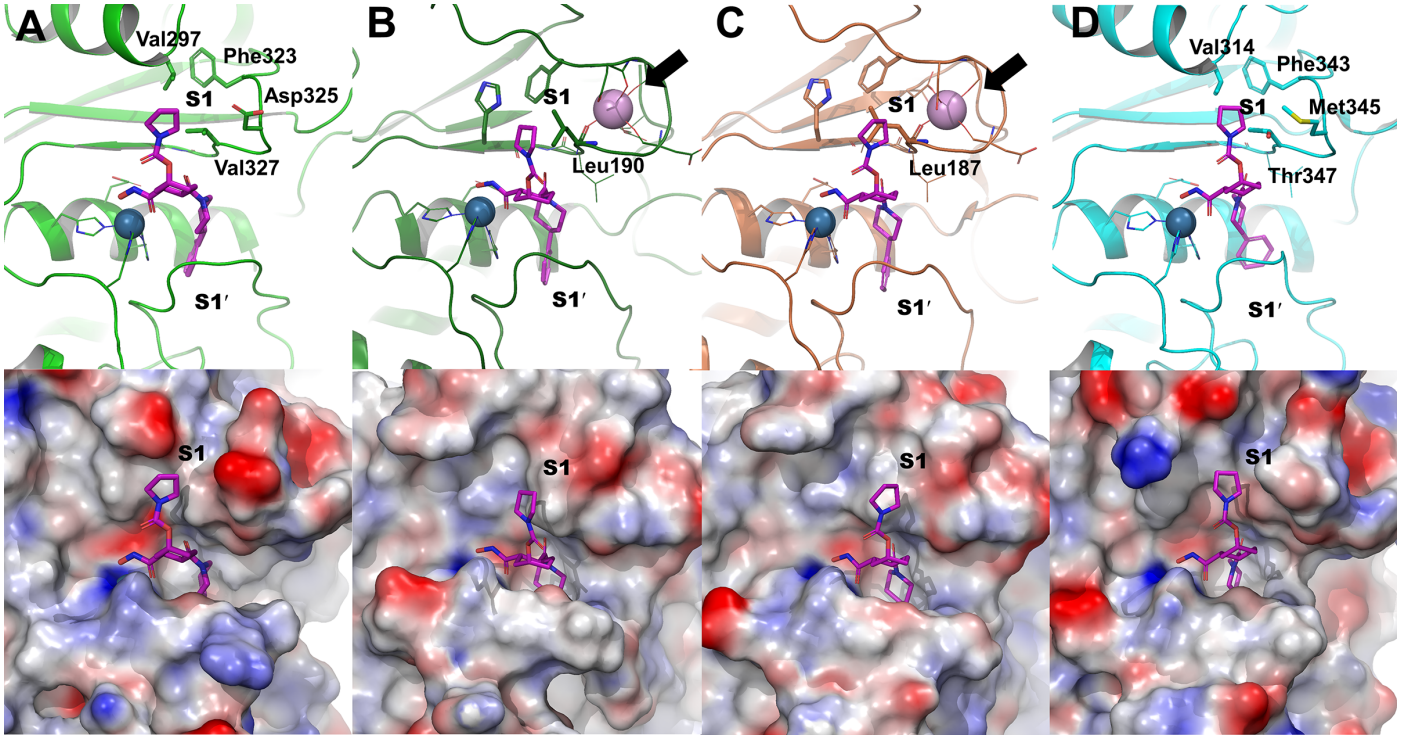


**Figure S5**. Compound **2** (represented in stick with purple color for carbon atoms) docked to the active sites of the X-ray structures of ADAM10 (A), MMP-2 (B), MMP-9 (C), and ADAM17 (D). Upper panel shows relevant amino acids (stick and line representations), ions (sphere representation) and protein (ribbon representation). The black arrows point to the calcium ions in MMPs (B and C). The lower panel shows surface representation for the protein in the same orientation as the upper panel. The surface is colored based on electrostatic potential with red for negative atomic partial charges and blue for positive charges. The S1 site differs in steric and electrostatic properties.

**Protein modeling**

The amino-acid sequence of the catalytic domain of ADAM10 was retrieved from the UniProt database (accession number: O14672). The sequence similarity search to the Protein Data Bank (rcsb.org) revealed ADAM17 as the most homologous available X-ray template structure (sequence identity and similarity of 35% and 52%, respectively). The sequence analysis showed that the structural alignment extended through the length of the catalytic domain, suggesting the ability to model the entire domain reliably. Coordinates of two ADAM17 X-ray structures were used in the modeling (PDB codes 1BKC and 3G42). Comparative modeling was performed with Modeler v 9.12.[11] A total of 100 models were built and ranked with DOPE scoring function. One model was selected from the top ten models after visual inspection of the binding site and was prepared with the Maestro program (v. 9.5, Schrödinger LLC, NY, USA). During the process, proper bond orders were assigned, disulfide bonds were created, and hydrogen atoms were added. Appropriate protonation states for the residues were assigned, followed by energy-minimization with the OPLS2005 forcefield.

**Synthesis**

Compounds were synthesized following previously reported protocol.[12, 13]

**(6*S*,7*S*)-*N*-hydroxy-5-methyl-6-(4-(5-(trifluoromethyl)pyridin-2-yl)piperazine-1-carbonyl)-5-azaspiro[2.5]octane-7-carboxamide.** (**1**). $^1$H NMR (500 MHz, MeOD-$d_4$) δ 0.57-0.54 (m, 3H), 0.74 (d, $J$ = 6.5 Hz, 1H), 1.20-1.17 (m, 1H), 2.30 (d, $J$ = 13.0 Hz, 1H), 2.63-2.53 (m, 3H), 2.90-2.84 (m, 1H), 3.82-3.59 (m, 9H), 4.32 (d, $J$ = 9.5 Hz , 1H), 6.92 (d, $J$ = 9.0 Hz, 1H), 7.36-7.32 (m, 1H), 7.76 (d, $J$ = 1.5 Hz, 1H), 8.37 (s, 1H). HRMS $[M + H]^+$, calcd for $C_{20}H_{27}F_3N_5O_3$ 442.2061; found 442.2048.

**(1*R*,3*S*,4*S*)-3-(hydroxycarbamoyl)-4-(4-phenylpiperidine-1-carbonyl)cyclohexyl pyrrolidine-1-carboxylate**. (**2**). $^1$H NMR (500 MHz, $CDCl_3$) δ 2.06-1.57 (m, 15H), 2.77-2.62 (m, 2H), 3.05-2.98 (m, 2H), 3.19-3.10 (m, 1H), 3.42-3.37 (m, 4H), 4.11-3.99 (m, 1H), 4.72 (d, $J$ = 7.5 Hz, 1H), 5.08 (s, 1H), 7.32-7.16 (m, 5H), 9.24 (s, 1H); HRMS $[M + Na]^+$, calcd for $C_{24}H_{33}N_3O_5Na$ 466.2312; found 466.2314.

**Purity**

The purity of compounds **1** and **2** was determined by UPLC with UV detection. A Waters Acquity UPLC system (Waters Corporation, Milford, MA, USA) equipped with a binary solvent manager, an autosampler, a column heater, and a photodiode array detector was used. The compounds were analyzed on a Kinetex C18 column (2.6 μm, 2.1 μm x 100 mm, Phenomenex, Torrance, CA, USA) at a column temperature of 48 °C . The mobile phase consisted of elution at 0.4 mL/min with 90% A/10% B for 2 min, followed by an 8-min linear gradient to 10% A/90% B, then 2 min with 90% A/10% B (A = water containing 0.1% formic acid, B = acetonitrile containing 0.1% formic acid). The effluent was monitored by UV detection at 260 nm and the area of the peaks was integrated. The purity of compounds **1** and **2** was ≥95%.

**Kinetics**

The enzymes, MMP-1, MMP-2, MMP-3, MMP-7, MMP-8, MMP-9, MMP-14, ADAM9 and ADAM10, and their corresponding substrates were obtained, as previously reported.[14] Recombinant human active TACE/ADAM17 was purchased from R&D Systems (Minneapolis, MN, USA); the catalytic domain of MMP-12 was purchased from Enzo Life Sciences, Inc. (Farmingdale, NY, USA). Mca-PLAQAV-Dpa-RSSSR-$NH_2$ (for ADAM17) and Mca-PLGL-Dpa-AR-$NH_2$ (for MMP-12) were purchased from R&D Systems (Minneapolis, MN, USA). Inhibitor stock solutions (10 mM) were prepared freshly in DMSO before enzyme inhibition assays. The enzyme inhibition studies were performed according to a previously reported protocol.[15] $K_i$ values were measured in triplicate. A Cary Eclipse fluorescence spectrophotometer (Varian, Walnut Creek, CA, USA) was used to conduct enzyme inhibition studies.

**Pharmacokinetics**

For ip administration, compound **2** was dissolved in 5% DMSO/15% propylene glycol/80% water at a concentration of 3 mg/mL. For sc administration, compound **2** was prepared in 10% DMSO/20% propylene glycol/70% water at a concentration of 7.5 mg/mL. The dosing formulations were sterilized by filtration through an Acrodisc syringe filter containing a PTFE membrane (2 μm, 13 mm diameter, Pall Life Sciences, Port Washington, NY). Blood and brain were collected at 5, 40, 120, 240, and 480 min after ip administration and at 20, 40, 60, 120, 240, and 480 min after sc administration.

Standard curves in control mouse plasma and brain were prepared as previously described.[14] One volume of plasma was mixed with two volumes of acetonitrile containing internal standard (final concentration 3 μM); the internal standard used was the same as previously reported.[14] The mixture was centrifuged at 10000 *g* for 15 min, and the supernatant was analyzed by UPLC on a reverse phase Acclaim RSLC120 C18 column (2.2 μm, 2.1 x 100 mm, Dionex, Sunnyvale, CA) with multiple-reaction monitoring (MRM) in electrospray ionization negative mode. The mass spectrometry conditions were the same as previously reported.[14] The MRM transitions used were 444 → 296 for compound **2** and 300 → 93 for the internal standard. Linear-regression parameters from the calibration curves were used to quantify compound **2** in plasma and brain using peak-area ratios relative to the internal standard. The coefficients of determination R2 were >0.99; the assays were linear up to a concentration of 100 μM.

## References:


(1) Yao, W.; Zhuo, J.; Burns, D. M.; Li, Y. L.; Qian, D. Q.; Zhang, C.; He, C.; Xu, M.; Shi, E.; Li, Y.; Marando, C. A.; Covington, M. B.; Yang, G.; Liu, X.; Pan, M.; Fridman, J. S.; Scherle, P.; Wasserman, Z. R.; Hollis, G.; Vaddi, K.; Yeleswaram, S.; Newton, R.; Friedman, S.; Metcalf, B. Design and identification of selective HER-2 sheddase inhibitors via P1' manipulation and unconventional P2' perturbations to induce a molecular metamorphosis. *Bioorg. Med. Chem. Lett.* **2008**, *18*, 159-163.

(2) Burns, D. M.; He, C.; Li, Y.; Scherle, P.; Liu, X.; Marando, C. A.; Covington, M. B.; Yang, G.; Pan, M.; Turner, S.; Fridman, J. S.; Hollis, G.; Vaddi, K.; Yeleswaram, S.; Newton, R.; Friedman, S.; Metcalf, B.; Yao, W. Conversion of an MMP-potent scaffold to an MMP-selective HER-2 sheddase inhibitor via scaffold hybridization and subtle P1' permutations. *Bioorg. Med. Chem. Lett.* **2008**, *18*, 560-564.

(3) Girijavallabhan, V. M.; Chen, L.; Dai, C.; Feltz, R. J.; Firmansjah, L.; Li, D.; Kim, S. H.; Kozlowski, J. A.; Lavey, B. J.; Kosinski, A.; Piwinski, J. J.; Popovici-Muller, J.; Rizvi, R.; Rosner, K. E.; Shankar, B. B.; Shih, N. Y.; Siddiqui, M. A.; Tong, L.; Wong, M. K.; Yang, D. Y.; Yang, L.; Yu, W.; Zhou, G.; Guo, Z.; Orth, P.; Madison, V.; Bian, H.; Lundell, D.; Niu, X.; Shah, H.; Sun, J.; Umland, S. Novel TNF-alpha converting enzyme (TACE) inhibitors as potential treatment for inflammatory diseases. *Bioorg. Med. Chem. Lett.* **2010**, *20*, 7283-7287.

(4) Rosner, K. E.; Guo, Z.; Orth, P.; Shipps, G. W., Jr.; Belanger, D. B.; Chan, T. Y.; Curran, P. J.; Dai, C.; Deng, Y.; Girijavallabhan, V. M.; Hong, L.; Lavey, B. J.; Lee, J. F.; Li, D.; Liu, Z.; Popovici-Muller, J.; Ting, P. C.; Vaccaro, H.; Wang, L.; Wang, T.; Yu, W.; Zhou, G.; Niu, X.; Sun, J.; Kozlowski, J. A.; Lundell, D. J.; Madison, V.; McKittrick, B.; Piwinski, J.

J.; Shih, N. Y.; Arshad Siddiqui, M.; Strickland, C. O. The discovery of novel tartrate-based TNF-alpha converting enzyme (TACE) inhibitors. *Bioorg. Med. Chem. Lett.* **2010**, *20*, 1189-1193.

(5) Gilson, M. K.; Liu, T.; Baitaluk, M.; Nicola, G.; Hwang, L.; Chong, J. BindingDB in 2015: A public database for medicinal chemistry, computational chemistry and systems pharmacology. *Nucleic Acids Res.* **2016**, *44*, D1045-1053.

(6) Halgren, T. A.; Murphy, R. B.; Friesner, R. A.; Beard, H. S.; Frye, L. L.; Pollard, W. T.; Banks, J. L. Glide: a new approach for rapid, accurate docking and scoring. 2. Enrichment factors in database screening. *J Med. Chem.* **2004**, *47*, 1750-1759.

(7) Burns, D. M.; Li, Y. L.; Shi, E.; He, C.; Xu, M.; Zhuo, J.; Zhang, C.; Qian, D. Q.; Li, Y.; Wynn, R.; Covington, M. B.; Katiyar, K.; Marando, C. A.; Fridman, J. S.; Scherle, P.; Friedman, S.; Metcalf, B.; Yao, W. Compelling P1 substituent affect on metalloprotease binding profile enables the design of a novel cyclohexyl core scaffold with excellent MMP selectivity and HER-2 sheddase inhibition. *Bioorg. Med. Chem. Lett.* **2009**, *19*, 3525-3530.

(8) Li, Y. L.; Shi, E.; Burns, D.; Li, Y.; Covington, M. B.; Pan, M.; Scherle, P.; Friedman, S.; Metcalf, B.; Yao, W. Discovery of novel selective HER-2 sheddase inhibitors through optimization of P1 moiety. *Bioorg. Med. Chem. Lett.* **2009**, *19*, 5037-5042.

(9) Liu, P. C.; Liu, X.; Li, Y.; Covington, M.; Wynn, R.; Huber, R.; Hillman, M.; Yang, G.; Ellis, D.; Marando, C.; Katiyar, K.; Bradley, J.; Abremski, K.; Stow, M.; Rupar, M.; Zhuo, J.; Li, Y. L.; Lin, Q.; Burns, D.; Xu, M.; Zhang, C.; Qian, D. Q.; He, C.; Sharief, V.; Weng, L.; Agrios, C.; Shi, E.; Metcalf, B.; Newton, R.; Friedman, S.; Yao, W.; Scherle, P.; Hollis, G.; Burn, T. C. Identification of ADAM10 as a major source of HER2 ectodomain sheddase activity in HER2 overexpressing breast cancer cells. *Cancer Biol. Ther.* **2006**, *5*, 657-664.

(10) Yao, W.; Zhuo, J.; Burns, D. M.; Xu, M.; Zhang, C.; Li, Y. L.; Qian, D. Q.; He, C.; Weng, L.; Shi, E.; Lin, Q.; Agrios, C.; Burn, T. C.; Caulder, E.; Covington, M. B.; Fridman, J. S.; Friedman, S.; Katiyar, K.; Hollis, G.; Li, Y.; Liu, C.; Liu, X.; Marando, C. A.; Newton, R.; Pan, M.; Scherle, P.; Taylor, N.; Vaddi, K.; Wasserman, Z. R.; Wynn, R.; Yeleswaram, S.; Jalluri, R.; Bower, M.; Zhou, B. B.; Metcalf, B. Discovery of a potent, selective, and orally active human epidermal growth factor receptor-2 sheddase inhibitor for the treatment of cancer. *J Med. Chem.* **2007**, *50*, 603-606.

(11) Eswar, N.; Webb, B.; Marti-Renom, M. A.; Madhusudhan, M. S.; Eramian, D.; Shen, M. Y.; Pieper, U.; Sali, A. Comparative protein structure modeling using MODELLER. *Curr. Protoc. Protein Sci.* **2007**, *Chapter 2*, Unit 2 9.

(12) Li, Y.-l.; Zhuo, J.; Burns, D.; Yao, W.; Jalluri, R. K. Substituted cyclic hydroxamates as inhibitors of matrix metalloproteinases. WO Patent 2005,037,826, April 28, 2005.

(13) Yao, W.; Zhuo, J.; Xu, M.; Zhang, F.; Metcalf, B. W. AZA spiro alkane derivatives as inhibitors of metalloproteases. WO Patent 2004,096,139, November 11, 2004.

(14) Gao, M.; Zhang, H.; Trivedi, A.; Mahasenan, K. V.; Schroeder, V. A.; Wolter, W. R.; Suckow, M. A.; Mobashery, S.; Noble-Haeusslein, L. J.; Chang, M. Selective Inhibition of MMP-2 Does Not Alter Neurological Recovery after Spinal Cord Injury. *ACS Chem. Neurosci.* **2016**, *7*, 1482-1487.

(15) Page-McCaw, A.; Ewald, A. J.; Werb, Z. Matrix metalloproteinases and the regulation of tissue remodelling. *Nat. Rev. Mol. Cell Bio.* **2007**, *8*, 221-233.